Hindawi
Mathematical Problems in Engineering
Volume 2019, Article ID 8709369, 9 pages
https://doi.org/10.1155/2019/8709369

Research Article

Backstepping Control Using Barrier Lyapunov Function for Dynamic Positioning Control System with Passive Observer

Guoqing Xia, Jingjing Xue, Chuang Sun, and Bo Zhao

College of Automation, Harbin Engineering University, Harbin, China

Correspondence should be addressed to Jingjing Xue; xuejingjing@hrbeu.edu.cn

Received 14 September 2018; Revised 17 December 2018; Accepted 13 January 2019; Published 3 February 2019

Academic Editor: Jorge Rivera

Copyright © 2019 Guoqing Xia et al. This is an open access article distributed under the Creative Commons Attribution License, which permits unrestricted use, distribution, and reproduction in any medium, provided the original work is properly cited.

This paper presents a backstepping controller using barrier Lyapunov function (BLF) for dynamic positioning (DP) system. For safety reasons, the position and heading of DP ship are to be maintained in certain range. Thus, in this paper, a control law based on BLF and backstepping technique is proposed to limit the position and heading. The closed-loop system is proved stable in the sense of Lyapunov stability theories. In addition, since the velocities of ship are not measurable and the wave frequency (WF) motion is unavailable, a passive observer is adopted to estimate the velocities and the effect of WF motion. The simulation results show that the proposed controller can limit the position and heading of the vessel in a predefined range and verify the performance of the proposed controller and the passive observer.

1. Introduction

With the exploration of ocean resources such as oil and gas, dynamic positioning (DP) control system is increasingly applied in deep sea drilling operations. The number of ships with DP control system has risen to thousands, and the trend continues. DP ship is defined as a ship that only depending on active thrusters maintains its position and heading (fixed location or predetermined track) (see [1] (Sørensen A J, 2011)). DP control system is a complex nonlinear system with uncertain disturbances, parameter uncertainties, input saturation, time-delay, and so on. Thus, the study of DP control system focuses on nonlinearity, unmodeled dynamics, unknown environmental disturbances, input saturation, time-delay, and so on (see [1–4] (Sørensen A J, 2005; 2011; Rabanal O M R, Brodtkorb A H, Breivik M, 2016; Xia G, Xue J, Jiao J et al., 2016)). Among those control strategies, backstepping method is a common technique to achieve a control law via defining error variables and a corresponding Lyapunov function of each subsystem to ensure system stability. The paper in [5] (Kim Y S, Kim J, Sung H G, 2016) applied nonlinear backstepping technique in weather-optimal controller designed for DP control system to maintain ship in a fixed position. The study in [6] (Xia, G., Xue, J., Jiao, J, 2018) combined backstepping technique with fuzzy approach to resolve the problem of time-delay and uncertainties in DP control system. The authors in [7] (Morishita H M, Souza C E S, 2014) developed an attenuating control law on basis of observer backstepping methodology for DP control system considering the saturation of actuators.

Moreover, in marine operation, the position of ship with DP control system shall be limited in certain range to ensure safe operation (see [2, 8] (Sørensen A J, 2005; Liu X, Abrahamsen B, 2010)). And the study of state constraints has drawn much attention in area of control system (see, for instance, [9–11] (Liu Y J, Tong S, 2016; 2017; Wei H, Zhao Y, Sun, 2017)). Using diffeomorphisms to transform nonlinear constrained control problem into an unconstrained one, the authors in [12] (Doria-Cerezo A, Acosta J A, Castano A R et al., 2014) applied nonlinear state and input constraints control theories to the DP control system to ensure safe operation. To ensure state constraints, BLF has been widely accepted as an effective scheme since this method needs less restrictive initial conditions comparing with other methods, such as reference setting method, model predictive control, and control theories based on invariant set or admissible set. In order to tackle the nonlinearities of control signals and guarantee a safe operation, the study in [13] (Tu F, Ge

S S, Choo Y S et al., 2017) presented an adaptive neural constrained control with nonlinear adaptive filter based on BLF for DP of an accommodation ship in deep water. To tackle the constraint problems, the study in [14] (Kong L, He W, Yang C et al., 2018) utilized an asymmetric time-varying BLF to the design of adaptive fuzzy neural network control, proved that closed-loop system was stable by Lyapunov stability theory, and verified the effectiveness of proposed control by comparative simulations. Combining the BLF with backstepping technique is one method of the application of BLF to tackle the problem of state constraint in control areas. For the purpose of solving the problem of the error constraint, the authors in [15] (Ghommam J, Ferik S E, Saad M, 2018) proposed a new robust adaptive controller incorporating tan-BLF with the backstepping control and guaranteed the proposed control law semi-global uniform ultimately bounded stability using Lyapunov stability theory. With the aim of solving the problem of output constraint, the study in [16] (Zheng Z, Huang Y, Xie L et al., 2018) combined an asymmetric time-varying BLF with backstepping technique, employed the hyperbolic tangent function to approximate the saturation function to overcome the input saturation, and verified the effectiveness of the proposed controller by simulation results.

In practice, the wave frequency (WF) motion of DP ship is the most interesting aspect of DP such as estimating the first order WF motions of the ship and excluding it from the feedback loop. In order to estimate the position, heading, and velocities of ship, the authors in [17] (Du J, Hu X, Liu H et al., 2015) proposed a high-gain observer and an adaptive robust output feedback control scheme to estimate velocities and unknown parameters. Using disturbance observer to estimate unknown time-varying disturbances, the study in [18] (Du J, Hu X, Krstić M et al., 2016) came up with a robust nonlinear control law for DP control system to handle input saturation. For the sake of improving performance of model-based observers for DP ship during transients, the authors in [19] (Svenn A. Værnø, Brodtkorb A H, Skjetne R et al., 2017) developed a model-based observer with time-varying gains, and the performance of designed observer was verified on research ship Gunnerus.

The main contribution of this paper is the design of a backstepping control law using BLF for DP control system. With this controller, the close-loop system is proved stable in the sense of Lyapunov stability, and the position of the vessel is guaranteed to be limited in a predefined range. Besides, a traditional backstepping control law is compared to the newly designed control law in order to intuitively reveal the advantages of the two control laws. In addition, since the velocities of DP ship are not measurable and the WF motion is unavailable, a passive observer is adopted to estimate the low frequency (LF) motion of DP ship and the effect of WF motion. The rest of the paper is organized as follows. Problem formulation is presented in Section 2. Using BLF, a backstepping control law is developed based on Lyapunov stability theories, the traditional backstepping control law is designed, and a passive observer is introduced in Section 3. The stability of designed control law is proved in Section 4. MATLAB simulation results demonstrate the effectiveness of the designed controller and observer in Section 5. Finally, the conclusion is summarized in Section 6.

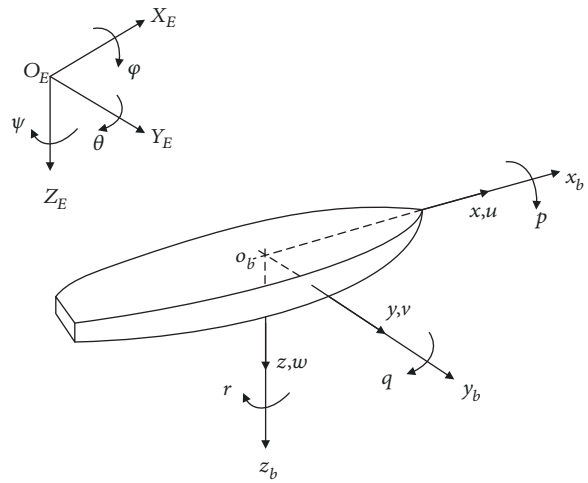

Figure 1: The reference frames.

2. Problem Formulation

This section describes the mathematical model of DP ship, and the control objective is introduced in this part.

2.1. The Kinematics and Dynamics of DP Ship. In order to analyze the dynamics of DP ship, the earth-fixed reference frame denoted as $O_E - X_E Y_E Z_E$ and body-fixed reference frame denoted as $o_b - x_b y_b z_b$ are introduced and shown in Figure 1.

As shown in Figure 1, ship motion is described in 6-degree-of-freedom (DOF) model including three-translational motion and three-rotational motion along the x_b-, y_b-, and z_b- axes. DP model can be derived under the assumption of low speed to keep position; it is widely accepted in the research of DP control system that only three-horizontal motion is considered. The position vector in earth-fixed reference is defined as $\boldsymbol{\eta} = [x, y, \psi]^{\mathrm{T}}$ and the velocity in body-fixed reference is defined as $\boldsymbol{v} = [u, v, r]^{\mathrm{T}}$. And the kinematics of DP ship is described as

$$\dot{\boldsymbol{\eta}} = \mathbf{R}(\psi)\boldsymbol{v} \tag{1}$$

where $\mathbf{R}(\psi)$ is the rotation matrix transforming body-fixed velocities into earth-fixed velocities with the properties of $\mathbf{R}^{-1}(\psi) = \mathbf{R}^{\mathrm{T}}(\psi)$, $\mathbf{R}(\psi)\mathbf{R}^{\mathrm{T}}(\psi) = I_{3\times3}$, $I_{n\times n}$ represents $n \times n$ identity matrix, and $\mathbf{R}(\psi)$ is expressed by

$$\mathbf{R}(\psi) = \begin{bmatrix} \cos(\psi) & \sin(\psi) & 0 \\ -\sin(\psi) & \cos(\psi) & 0 \\ 0 & 0 & 1 \end{bmatrix} \tag{2}$$

In DP control system, the model of ship is often separated into LW model and WF model (see [20] (Fossen, T. I, 2002)).

The 3-DOF model of DP ship in LF motion and WF motion is written as

$$\begin{aligned}\dot{\boldsymbol{\xi}}_w &= \mathbf{A}_w\boldsymbol{\xi}_w + \mathbf{E}_w\mathbf{w}_w\\ \dot{\boldsymbol{\eta}} &= \mathbf{R}(\psi)\boldsymbol{v}\\ \dot{\mathbf{b}} &= -T^{-1}\mathbf{b}\\ \dot{\boldsymbol{v}} &= \mathbf{M}^{-1}\left(-\mathbf{D}\boldsymbol{v} + \boldsymbol{\tau}_c + \mathbf{R}^{\mathrm{T}}(\psi)\mathbf{b}\right)\\ \mathbf{y} &= \boldsymbol{\eta} + \mathbf{C}_w\boldsymbol{\xi}_w\end{aligned} \tag{3}$$

where $\boldsymbol{\xi}_w \in \mathfrak{R}^6$ is the WF motion state vector; $\mathbf{A}_w \in \mathfrak{R}^{6\times6}$, $\mathbf{E}_w \in \mathfrak{R}^{6\times3}$ and $\mathbf{C}_w \in \mathfrak{R}^{3\times6}$ are the constant matrices; $\mathbf{w}_w \in \mathfrak{R}^3$ represents the zero-mean Gaussian white noise; $\boldsymbol{\eta}_w \in \mathfrak{R}^3$ is position and orientation vector due to one-order wave-induced motion; $\mathbf{M} \in \mathfrak{R}^{3\times3}$, $\dot{\mathbf{M}} = \mathbf{0}$ is the total matrix including inertia mass matrix and added mass matrix; $\mathbf{D} \in \mathfrak{R}^{3\times3}$ is the hydrodynamic damping matrix; $\boldsymbol{\tau}_c \in \mathfrak{R}^3$ is control force caused by the thrusters of DP ship; $\mathbf{b} \in \mathfrak{R}^3$ is environmental disturbances such as wind, waves, and ocean currents and can be determined by formulas of environmental forces; $\mathbf{y} \in \mathfrak{R}^{3\times3}$ is the measurement vector, and $\mathbf{C}_w \in \mathfrak{R}^{3\times6}$ is constant matrix.

2.2. Control Objective. For DP ship, the horizontal displacement of DP ship should be maintained in certain range in order to ensure safety operation. That is, the position in surge and sway should be limited such as $|x| \le x_{\lim}$, $|y| \le y_{\lim}$ and the yaw angle is always in region of $(-\psi_{\max}, \psi_{\max})$. One control objective is to design a control law that steers ships to the desired position and heading in the condition of constrained position and heading with the environmental disturbances. The other objective is the designed control law maintaining the position and head of ship at the desired position, heading in the condition of constrained position, and heading under the effect of environmental disturbances.

3. Backstepping Control Using BLF

In this section, the backstepping control law is to be designed using BLF to steer DP ship to the desired position and heading under state constraints and disturbances. And the close-loop system of the proposed control scheme is proved stable in sense of Lyapunov stability theories. The traditional backstepping control law is compared to the proposed control law with BLF in this section. Moreover, a passive observer is adopted in this section to estimate the available and unavailable states of DP control system.

3.1. Backstepping Control Law Using BLF. The basic knowledge of BLF is introduced before designing the control law.

Definition 1 (see [21, 22] (Zhang T, Wang N, Xia M., 2017; Ren B, Ge S S, Tee K P et al., 2010)). A BLF is a scalar function $V(x)$, defined with respect to the system $\dot{x} = f(x)$ on an open region D containing the origin; BLF is continuous, positive definite and has continuous first-order partial derivatives at every point of D; the BLF has the property that $V(x) \longrightarrow \infty$ as x approaches the boundary of D and satisfies $V(x(t)) \le b, \forall t \ge 0$, along the solution of $\dot{x} = f(x)$ with $x(0) \in D$ and some positive constant b.

In this paper, the BLF is chosen as

$$V(x) = \frac{1}{2}\ln\frac{k^2}{k^2 - z^2} \tag{4}$$

where z is the error; k is the positive constraint value on z; that is $|z| \le k$.

Lemma 2 (see [21, 22] (Zhang T, Wang N, Xia M., 2017; Ren B, Ge S S, Tee K P et al., 2010)). *For any positive constant k_{b1}, let $\mathbb{Z}_1 := \{z \in \mathfrak{R} \mid |z| < k\} \subset \mathfrak{R}$ and $\mathbb{N} := \mathfrak{R}^l \times \mathbb{Z}_1 \subset \mathfrak{R}^{l+1}$ be open sets. Consider the system*

$$\phi = h(t, \phi) \tag{5}$$

where $\phi := [\omega, z]^{\mathrm{T}} \in \mathbb{N}(\omega \in \mathfrak{R}^l)$ is the state and function $h := \mathfrak{R}^+ \times \mathbb{N} \longrightarrow \mathfrak{R}^{l+1}$ is piecewise continuous in t and locally Lipschitz in z, uniformly in t on $\mathfrak{R}^+ \times \mathbb{N}$. Supposing that there exist two continuously differentiable and positive definite functions $U : \mathfrak{R}^l \longrightarrow \mathfrak{R}^+$ and $V_1 : \mathbb{Z} \longrightarrow \mathfrak{R}^+$ in their respective domain, so that

$$\begin{gathered}V_1(z) \longrightarrow \infty, \quad |z| \longrightarrow k\\ \beta_1(\|\omega\|) \le U(\omega) \le \beta_2(\|\omega\|)\end{gathered} \tag{6}$$

where β_1, β_2 are class K_∞ functions. Let $z(0) \in \mathbb{Z}_1$ and $V(\phi) := V_1(z) + U(\omega)$. If the following inequality establishes

$$\dot{V} = \frac{\partial V}{\partial \phi}h \le -\mu V + \lambda \tag{7}$$

where μ and λ are positive constants, then ω remains bounded and $z(t) \in \mathbb{Z}_1, \forall t \in [0, \infty)$.

Lemma 3 (see [22] (Ren B, Ge S S, Tee K P et al., 2010)). *For any constant $k > 0$, when $|z| \le k$, the following inequation is held:*

$$\ln\frac{k^2}{k^2 - z^2} < \frac{k^2}{k^2 - z^2} \tag{8}$$

Based on the above introduction, expanding the one-dimensional theory of BLF into three-dimension, a recursive backstepping control law based on BLF is designed in the following steps.

Step 1. The desired position and heading vector is defined as $\boldsymbol{\eta}_d \in \mathfrak{R}^3$. And the position and heading error variable is defined as

$$\mathbf{z}_1 = \boldsymbol{\eta} - \boldsymbol{\eta}_d = \left[z_x, z_y, z_\psi\right]^{\mathrm{T}} \tag{9}$$

Combining with (1) and (9), the time derivate of $\mathbf{z}_1$ is derived as

$$\dot{\mathbf{z}}_1 = \dot{\boldsymbol{\eta}} - \dot{\boldsymbol{\eta}}_d = \mathbf{R}(\psi)\boldsymbol{v} - \dot{\boldsymbol{\eta}}_d \tag{10}$$

And the virtual control law $\boldsymbol{\alpha}_{21} \in \Re^3$ is designed as

$$\boldsymbol{\alpha}_{21} = -\left(\mathbf{k}_1^{\mathrm{T}}\mathbf{k}_1 - \mathbf{z}_1^{\mathrm{T}}\mathbf{z}_1\right)\mathbf{R}^{\mathrm{T}}(\psi)K_{21}\mathbf{z}_1 + \mathbf{R}^{\mathrm{T}}(\psi)\dot{\boldsymbol{\eta}}_d \tag{11}$$

where $\mathbf{k}_1 \in \Re^3$ is positive constant vector and it is the constraint condition on $\mathbf{z}_1$, and $K_{21} \in \Re^{3\times3}$ is a positive definite and diagonal matrix.

Step 2. The velocity error variable is defined as

$$\mathbf{z}_2 = \boldsymbol{v} - \boldsymbol{\alpha}_{21} = [z_u, z_v, z_r]^{\mathrm{T}} \tag{12}$$

So (10) is rewritten as

$$\dot{\mathbf{z}}_1 = \mathbf{R}(\psi)(\mathbf{z}_2 + \boldsymbol{\alpha}_{21}) - \dot{\boldsymbol{\eta}}_d \tag{13}$$

Combining with (3) and (12), the time derivate of $\mathbf{z}_2$ is derived as

$$\dot{\mathbf{z}}_2 = \dot{\boldsymbol{v}} - \dot{\boldsymbol{\alpha}}_{21} = \mathbf{M}^{-1}\left(-\mathbf{D}\boldsymbol{v} - \mathbf{M}\dot{\boldsymbol{\alpha}}_{21} + \boldsymbol{\tau} + \mathbf{R}^{\mathrm{T}}(\psi)\mathbf{b}\right) \tag{14}$$

where $\dot{\boldsymbol{\alpha}}_{21}$ is the time derivate of $\boldsymbol{\alpha}_{21}$ and is computed as

$$\begin{aligned}\dot{\boldsymbol{\alpha}}_{21} = {} & 2\mathbf{z}_1^{\mathrm{T}}\dot{\mathbf{z}}_1\mathbf{R}^{\mathrm{T}}(\psi)K_{21}\mathbf{z}_1 \\ & - \left(\mathbf{k}_1^{\mathrm{T}}\mathbf{k}_1 - \mathbf{z}_1^{\mathrm{T}}\mathbf{z}_1\right)\dot{\mathbf{R}}^{\mathrm{T}}(\psi)K_{21}\mathbf{z}_1 \\ & - \left(\mathbf{k}_1^{\mathrm{T}}\mathbf{k}_1 - \mathbf{z}_1^{\mathrm{T}}\mathbf{z}_1\right)\mathbf{R}^{\mathrm{T}}(\psi)K_{21}\dot{\mathbf{z}}_1 + \dot{\mathbf{R}}^{\mathrm{T}}(\psi)\dot{\boldsymbol{\eta}}_d \\ & + \dot{\mathbf{R}}^{\mathrm{T}}(\psi)\ddot{\boldsymbol{\eta}}_d\end{aligned} \tag{15}$$

In view of the BLF theory to solve the problem of state constraint, thus the BLF is utilised into the design of control law. Therefore, the control law $\boldsymbol{\tau}_{blf} \in \Re^3$ is designed as

$$\begin{aligned}\boldsymbol{\tau}_{blf} = {} & -\frac{\mathbf{R}^{\mathrm{T}}(\psi)\mathbf{z}_1}{\mathbf{k}_1^{\mathrm{T}}\mathbf{k}_1 - \mathbf{z}_1^{\mathrm{T}}\mathbf{z}_1} + \mathbf{D}\boldsymbol{v} + \mathbf{M}\dot{\boldsymbol{\alpha}}_{21} - \mathbf{R}^{\mathrm{T}}(\psi)\mathbf{b} \\ & - K_{22}\mathbf{z}_2\end{aligned} \tag{16}$$

where $-(\mathbf{R}^{\mathrm{T}}(\psi)\mathbf{z}_1/(\mathbf{k}_1^{\mathrm{T}}\mathbf{k}_1 - \mathbf{z}_1^{\mathrm{T}}\mathbf{z}_1))$ is the item based on BLF to handle with the problem of state constraint, and $K_{22} \in \Re^{3\times3}$ is a positive definite and diagonal matrix.

3.2. Traditional Backstepping Control Law. The traditional backstepping control law [20, (Fossen, T. I, 2002)] is designed in the following steps.

Step 1. The position error is considered as $\mathbf{e}_1 = [e_x, e_y, e_\psi]^{\mathrm{T}}$, and the error dynamics is defined as

$$\mathbf{e}_1 = \boldsymbol{\eta}_1 - \boldsymbol{\eta}_d \tag{17}$$

where $\boldsymbol{\eta}_1 = [x_1, y_1, \psi_1]^{\mathrm{T}}$, $\boldsymbol{v}_1 = [u_1, v_1, r_1]^{\mathrm{T}}$ are the position and velocity vectors, respectively.

Combining with (1) and (17), the time derivate of $\mathbf{e}_1$ is determined as

$$\dot{\mathbf{e}}_1 = \dot{\boldsymbol{\eta}}_1 - \dot{\boldsymbol{\eta}}_d = \mathbf{R}(\psi)\boldsymbol{v}_1 - \dot{\boldsymbol{\eta}}_d \tag{18}$$

Thus, the virtual control vector $\boldsymbol{\alpha}_{11} \in \Re^3$ is chosen as

$$\boldsymbol{\alpha}_{11} = \mathbf{R}^{\mathrm{T}}(\psi)(\dot{\boldsymbol{\eta}}_d - K_{11}\mathbf{e}_1) \tag{19}$$

where $K_{11} \in \Re^{3\times3}$ is a positive definite and diagonal matrix.

Step 2. The velocity error is defined as $\mathbf{e}_2 = [e_u, e_v, e_r]^{\mathrm{T}}$, and the error dynamics is defined as

$$\mathbf{e}_2 = \boldsymbol{v}_1 - \boldsymbol{\alpha}_{11} \tag{20}$$

Combining with (3) and (20), the time derivate of $\mathbf{e}_2$ is derived as

$$\dot{\mathbf{e}}_2 = \boldsymbol{v}_1 - \boldsymbol{\alpha}_{11} = \mathbf{M}^{-1}\left(-\mathbf{D}\boldsymbol{v}_1 - \mathbf{M}\dot{\boldsymbol{\alpha}}_{11} + \boldsymbol{\tau} + \mathbf{R}^{\mathrm{T}}(\psi)\mathbf{b}\right) \tag{21}$$

Combining with (18) and (19), the time derivate of $\boldsymbol{\alpha}_{11}$ is determined as

$$\dot{\boldsymbol{\alpha}}_{11} = \dot{\mathbf{R}}^{\mathrm{T}}(\psi)(\dot{\boldsymbol{\eta}}_d - K_{11}\mathbf{e}_1) + \mathbf{R}^{\mathrm{T}}(\psi)(\ddot{\boldsymbol{\eta}}_d - K_{11}\dot{\mathbf{e}}_1) \tag{22}$$

And the traditional backstepping control law $\boldsymbol{\tau} \in \Re^3$ is designed as

$$\boldsymbol{\tau} = M\dot{\boldsymbol{\alpha}}_{11} + D\boldsymbol{v}_1 - K_{12}\mathbf{e}_2 - \mathbf{R}^{T}(\psi)\mathbf{e}_1 - \mathbf{R}^{\mathrm{T}}(\psi)\mathbf{b} \tag{23}$$

where parameter matrix $K_{12} \in \Re^{3\times3}$ is a positive definite and diagonal matrix.

3.3. Passive Observer. For DP ship, the velocities are not measurable and the WF motion is unavailable and this is necessary in controller designing. In order to obtain the changing tendency of the velocities and the effect of WF motion, a passive observer is adopted in this section [20, (Fossen, T. I, 2002)].

The passive observer is expressed as

$$\begin{aligned}\dot{\hat{\boldsymbol{\xi}}}_w &= \mathbf{A}_w\hat{\boldsymbol{\xi}}_w + K_1\tilde{\mathbf{y}} \\ \dot{\hat{\boldsymbol{\eta}}} &= \mathbf{R}(\psi_y)\hat{\boldsymbol{v}} + K_2\tilde{\mathbf{y}} \\ \dot{\hat{\mathbf{b}}} &= -T^{-1}\hat{\mathbf{b}} + K_3\tilde{\mathbf{y}} \\ \dot{\hat{\boldsymbol{v}}} &= \mathbf{M}^{-1}\left(-\mathbf{D}\hat{\boldsymbol{v}} + \boldsymbol{\tau}_c + \mathbf{R}^{\mathrm{T}}(\psi_y)\hat{\mathbf{b}}\right) + \mathbf{R}^{\mathrm{T}}(\psi_y)K_4\tilde{\mathbf{y}} \\ \hat{\mathbf{y}} &= \hat{\boldsymbol{\eta}} + \mathbf{C}_w\hat{\boldsymbol{\xi}}_w\end{aligned} \tag{24}$$

where $\hat{\boldsymbol{\xi}}_w, \hat{\boldsymbol{\eta}}, \hat{\mathbf{b}}, \hat{\boldsymbol{v}}$ are the estimation state vectors; $\mathbf{A}_w$ is the observer matrix and $K_1 \in \Re^{6\times3}$, $K_2, K_3, K_4 \in \Re^{3\times3}$ are the gain matrices; $\tilde{\boldsymbol{y}} = \boldsymbol{y} - \hat{\boldsymbol{y}}$ is the vector of estimation error; and ψ_y is the element of vector $\mathbf{y}$. And the passive observer was guaranteed uniformly globally exponential stability detailed in [20, (Fossen, T. I, 2002)].

4. Stability Analysis

4.1. Stability Analysis for Backstepping Control Law Using BLF. Based on the above introduction of BLF, the first BLF candidate V_{21} is chosen as

$$V_{21} = \frac{1}{2}\ln\frac{\mathbf{k}_1^{\mathrm{T}}\mathbf{k}_1}{\mathbf{k}_1^{\mathrm{T}}\mathbf{k}_1 - \mathbf{z}_1^{\mathrm{T}}\mathbf{z}_1} \tag{25}$$

So, the time derivate of V_{21} is derived by combining with (9), (12), and (25) as

$$\dot{V}_{21} = \frac{\mathbf{z}_1^{\mathrm{T}}\dot{\mathbf{z}}_1}{\mathbf{k}_1^{\mathrm{T}}\mathbf{k}_1 - \mathbf{z}_1^{\mathrm{T}}\mathbf{z}_1} = \frac{\mathbf{z}_1^{\mathrm{T}}\left(\mathbf{R}(\psi)(\mathbf{z}_2 + \boldsymbol{\alpha}_{21}) - \dot{\boldsymbol{\eta}}_d\right)}{\mathbf{k}_1^{\mathrm{T}}\mathbf{k}_1 - \mathbf{z}_1^{\mathrm{T}}\mathbf{z}_1} \tag{26}$$

Substituting (11) into (26), $\dot{V}_{21}$ can be rewritten as

$$\dot{V}_{21} = -\mathbf{z}_1^{\mathrm{T}}K_{21}\mathbf{z}_1 + \frac{\mathbf{z}_1^{\mathrm{T}}\mathbf{R}(\psi)\mathbf{z}_2}{\mathbf{k}_1^{\mathrm{T}}\mathbf{k}_1 - \mathbf{z}_1^{\mathrm{T}}\mathbf{z}_1} \tag{27}$$

According to the positive definite property of K_{21}, $\dot{V}_{21} = -\mathbf{z}_1^{\mathrm{T}}K_{21}\mathbf{z}_1 \leq 0$ when $\mathbf{z}_2$ is zero, thus, the variable of $\mathbf{z}_1$ is stabilization.

The second Lyapunov function candidate V_{22} is chosen as

$$V_{22} = V_{21} + \frac{1}{2}\mathbf{z}_2^{\mathrm{T}}\mathbf{M}\mathbf{z}_2 \tag{28}$$

So the time derivate of V_{22} is determined as

$$\dot{V}_{22} = \dot{V}_{21} + \frac{1}{2}\mathbf{z}_2^{\mathrm{T}}\dot{\mathbf{M}}\mathbf{z}_2 + \mathbf{z}_2^{\mathrm{T}}\mathbf{M}\dot{\mathbf{z}}_2 \tag{29}$$

Substituting (10), (27) into (29), $\dot{V}_{22}$ is derived as

$$\begin{aligned}\dot{V}_{22} = {} & -\mathbf{z}_1^{\mathrm{T}}K_{21}\mathbf{z}_1 + \frac{\mathbf{z}_1^{\mathrm{T}}\mathbf{R}(\psi)\mathbf{z}_2}{\mathbf{k}_1^{\mathrm{T}}\mathbf{k}_1 - \mathbf{z}_1^{\mathrm{T}}\mathbf{z}_1} + \frac{1}{2}\mathbf{z}_2^{\mathrm{T}}\dot{\mathbf{M}}\mathbf{z}_2 \\ & + \mathbf{z}_2^{\mathrm{T}}\left(-\mathbf{D}\boldsymbol{v} - \mathbf{M}\dot{\boldsymbol{\alpha}}_{21} + \boldsymbol{\tau} + \mathbf{R}^{\mathrm{T}}(\psi)\mathbf{b}\right)\end{aligned} \tag{30}$$

Due to the fact that mass matrix $\mathbf{M}$ is skew symmetric matrix and $\dot{\mathbf{M}} = \mathbf{0}$, thus, $\mathbf{z}_2^{\mathrm{T}}\dot{\mathbf{M}}\mathbf{z}_2 = 0$; therefore, $\dot{V}_{22}$ is rewritten as

$$\begin{aligned}\dot{V}_{22} = {} & -\mathbf{z}_1^{\mathrm{T}}K_{21}\mathbf{z}_1 + \frac{\mathbf{z}_1^{\mathrm{T}}\mathbf{R}(\psi)\mathbf{z}_2}{\mathbf{k}_1^{\mathrm{T}}\mathbf{k}_1 - \mathbf{z}_1^{\mathrm{T}}\mathbf{z}_1} \\ & + \mathbf{z}_2^{\mathrm{T}}\left(-\mathbf{D}\boldsymbol{v} - \mathbf{M}\dot{\boldsymbol{\alpha}}_{21} + \boldsymbol{\tau} + \mathbf{R}^{\mathrm{T}}(\psi)\mathbf{b}\right)\end{aligned} \tag{31}$$

Substituting the designed control law (16) into (30), $\dot{V}_{22}$ is determined as

$$\dot{V}_{22} = -\mathbf{z}_1^{\mathrm{T}}K_{21}\mathbf{z}_1 - \mathbf{z}_2^{\mathrm{T}}K_{22}\mathbf{z}_2 \tag{32}$$

So the variable of $\mathbf{z}_2$ is stabilization when $\dot{V}_2 \leq 0$. Therefore, the close-loop system under control of proposed control law $\boldsymbol{\tau}_{blf}$ is stable in the condition of constrained position and heading.

4.2. Stability Analysis for Traditional Backstepping Control Law. The Lyapunov function candidate V_{11} is selected as

$$V_{11} = \frac{1}{2}\mathbf{e}_1^{\mathrm{T}}\mathbf{e}_1 \tag{33}$$

Combining with (17), (18), and (20), the time derivate of V_{11} is computed as

$$\dot{V}_{11} = \mathbf{e}_1^{\mathrm{T}}\dot{\mathbf{e}}_1 = \mathbf{e}_1^{\mathrm{T}}\left(\mathbf{R}(\psi)(\mathbf{e}_2 + \boldsymbol{\alpha}_{11}) - \dot{\boldsymbol{\eta}}_d\right) \tag{34}$$

Substituting (19) into (34), $\dot{V}_{11}$ is determined as

$$\dot{V}_{11} = -\mathbf{e}_1^{\mathrm{T}}K_{11}\mathbf{e}_1 + \mathbf{e}_1^{\mathrm{T}}\mathbf{R}(\psi)\mathbf{e}_2 \tag{35}$$

Due to positive definite property of K_{21}, thus $\dot{V}_{11} = -\mathbf{e}_1^{\mathrm{T}}K_{11}\mathbf{e}_1 \leq 0$ when $\mathbf{e}_2$ is zero. Therefore, the variable of $\mathbf{e}_1$ is stabilization.

The Lyapunov function candidate V_{12} is selected as

$$V_{12} = V_{11} + \frac{1}{2}\mathbf{e}_2^{\mathrm{T}}\mathbf{M}\mathbf{e}_2 \tag{36}$$

So the time derivate of V_{12} is determined as

$$\dot{V}_{12} = \dot{V}_{11} + \frac{1}{2}\mathbf{e}_2^{\mathrm{T}}\dot{\mathbf{M}}\mathbf{e}_2 + \mathbf{e}_2^{\mathrm{T}}\mathbf{M}\dot{\mathbf{e}}_2 \tag{37}$$

Substituting (18), (21), and (35) into (37), $\dot{V}_{22}$ is derived as

$$\begin{aligned}\dot{V}_{22} = {} & -\mathbf{e}_1^{\mathrm{T}}K_{11}\mathbf{e}_1 + \mathbf{e}_1^{\mathrm{T}}\mathbf{R}(\psi)\mathbf{e}_2 \\ & + \mathbf{e}_2^{\mathrm{T}}\left(-\mathbf{D}\boldsymbol{v}_1 - \mathbf{M}\dot{\boldsymbol{\alpha}}_{11} + \boldsymbol{\tau} + \mathbf{R}^{\mathrm{T}}(\psi)\mathbf{b}\right)\end{aligned} \tag{38}$$

Substituting (23) into (38), $\dot{V}_{22}$ is determined as

$$\dot{V}_{12} = -\mathbf{e}_1^{\mathrm{T}}K_{11}\mathbf{e}_1 - \mathbf{e}_2^{\mathrm{T}}K_{12}\mathbf{e}_2 \leq 0 \tag{39}$$

Therefore, the variable of $\mathbf{z}_2$ is stabilization when $\dot{V}_2 \leq 0$. So the control system under traditional control law is stability.

5. Simulation Study

Based on LF motion of DP ship in Section 2, the mass matrix $\mathbf{M}$ of ship introduced in (3) is given as

$$\mathbf{M} = \begin{bmatrix} 9.1948 \times 10^7 & 0 & 0 \\ 0 & 9.1948 \times 10^7 & 9.6979 \times 10^8 \\ 0 & 9.6979 \times 10^8 & 1.0724 \times 10^{11} \end{bmatrix} \tag{40}$$

The damping matrix $\mathbf{D}$ of ship introduced in (3) is given as

$$\mathbf{D} = \begin{bmatrix} 1.5073 \times 10^6 & 0 & 0 \\ 0 & 8.1687 \times 10^6 & 9.6979 \times 10^8 \\ 0 & 9.6979 \times 10^8 & 1.2568 \times 10^{11} \end{bmatrix} \tag{41}$$

The desired position and heading are chosen as $\boldsymbol{\eta}_{d0} = [40m, 20m, 5^\circ]^{\mathrm{T}}$. The expected position is defined as $\boldsymbol{\eta}_d = [x_d, y_d, \psi_d]^{\mathrm{T}}$ and the expected velocity is defined as $\boldsymbol{v}_d = [u_d, v_d, r_d]^{\mathrm{T}}$. The initial values of position and heading vector are zero, and the original values of velocity vector are zero.

Thus, to generate a smooth desired path, the 2-order filter [20, (Fossen, T. I, 2002)] is adopted as

$$\begin{aligned}\dot{\boldsymbol{\eta}}_d &= \boldsymbol{v}_d \\ \ddot{\boldsymbol{\eta}}_d &= \omega^2{}_n\boldsymbol{\eta}_{d0} - \omega^2{}_n\boldsymbol{\eta}_d - \delta\left|\boldsymbol{\eta}_d\right|\boldsymbol{\eta}_d - 2\zeta\omega_n\boldsymbol{\eta}_d\end{aligned} \tag{42}$$

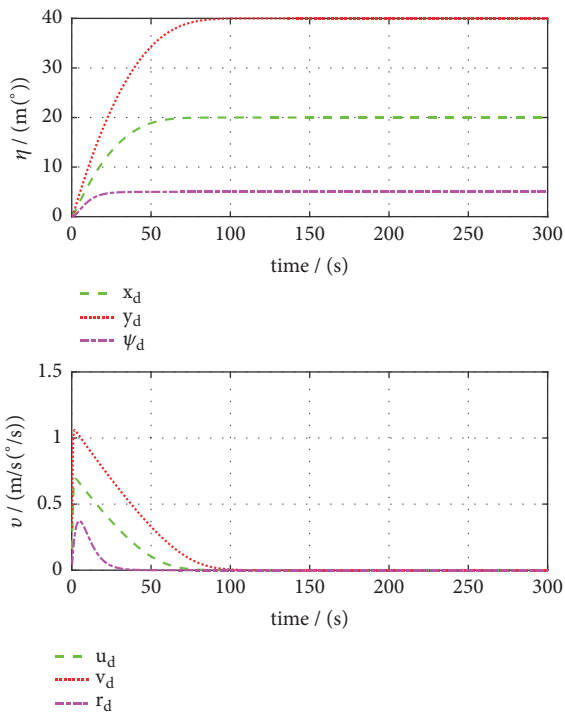

FIGURE 2: Time history of desired position and heading.

where ω_n is the natural frequency, ζ is the relative damping ratio, and δ is the designed parameter. In simulation, ω_n, ζ, and δ are chosen as $\omega_n = 0.2rad/s$, $\zeta = 1$, $\delta = 1$. Thus the desired states $\boldsymbol{\eta}_d, \boldsymbol{v}_d$ are generated smoothly and the figure of the desired states is shown in Figure 2. The desired position, desired heading, and desired velocities in three directions are smooth and converged to the given value of $\boldsymbol{\eta}_{d0}$ within $100s$. Besides, the bias term $\mathbf{b}$ introduced in (3) including wind, waves, and ocean currents disturbances is computed in [6, 20] (Xia, G., Xue, J., Jiao, J, 2018, Fossen, T. I, 2002).

What is more, the constant vector $\mathbf{k}_1$ considered in Section 3.1 is chosen as $\mathbf{k}_1 = [10.5m, 10.5m, 7.5^\circ]^{\mathrm{T}}$, which means that the position error of ship is allowed to move within a square with a side length of $10.5m$ and the heading error of the ship may vary within 7.5° range. And the gain matrices of backstepping control using BLF mentioned in Section 3.1 are chosen as

$$\begin{aligned} K_{21} &= \operatorname{diag}\left\{5\times10^{-3}, 1.4\times10^{-3}, 1\times10^{-2}\right\} \\ K_{22} &= \operatorname{diag}\left\{5\times10^{7}, 8.2\times10^{7}, 2.5\times10^{9}\right\} \end{aligned} \tag{43}$$

The gain matrices of traditional backstepping control introduced in Section 3.2 are listed as

$$\begin{aligned} K_{11} &= \operatorname{diag}\{0.8, 0.6, 0.8\} \\ K_{12} &= \operatorname{diag}\left\{5\times10^{7}, 5\times10^{8}, 9\times10^{9}\right\} \end{aligned} \tag{44}$$

The parameters in passive observer introduced in Section 3.3 are selected as

$$\begin{aligned} K_1 &= \operatorname{diag}\{-2.2, -2.2, -2.2, 1.6, 1.6, 1.6\}, \\ K_2 &= \operatorname{diag}\{1.1, 1.1, 1.1\}, \\ K_3 &= \operatorname{diag}\left\{3.3\times10^{5}, 3.3\times10^{5}, 1.9\times10^{8}\right\}, \\ K_4 &= \operatorname{diag}\left\{1\times10^{7}, 8\times10^{7}, 6.2\times10^{9}\right\} \end{aligned} \tag{45}$$

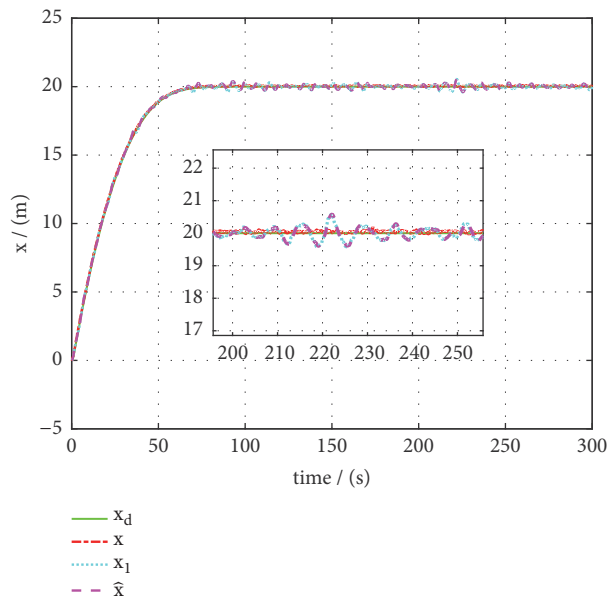

FIGURE 3: Time history of x-direction position.

There are four groups of simulation results in every element of position and velocity vectors: one group is the desired position, desired heading, and desired velocities with green solid line; the other one is under presented controller $\boldsymbol{\tau}_{blf}$ with red chain dotted line; the third one is under traditional controller $\boldsymbol{\tau}$ with cyan dotted line; and last one is under passive observer with red dashed line shown in Figures 3, 4, 5, 6, 7, and 8.

Figures 3, 4, and 5 are the time history of position in three directions. From Figure 3, position x smoothly moves along the desired position x_d in the condition of constrained positon from $\mathbf{k}_1$ and environmental disturbances. And the position x maintains at the desired position under the effect of environmental disturbances. Thus, the two control objectives are implemented under the control law $\boldsymbol{\tau}_{blf}$. Also position x_1 smoothly and precisely moves to the desired positon and maintains the desired position. And the estimated state $\hat{x}$ precisely and smoothly approaches the position in x-direction. But from the partial enlarged details in Figure 3, since the WF motion in x-direction is nonlinear motion and affects the whole motion of ship, the states x, x_1 and estimated state $\hat{x}$ oscillate slightly. However, x is smoother and more precise than x_1. In this view, the x-direction position under presented control law $\boldsymbol{\tau}_{blf}$ is more precise than under traditional control law $\boldsymbol{\tau}$.

With the same situation of Figure 4, position y smoothly moves along the desired position y_d in the condition of constrained positon from $\mathbf{k}_1$ and environmental disturbances

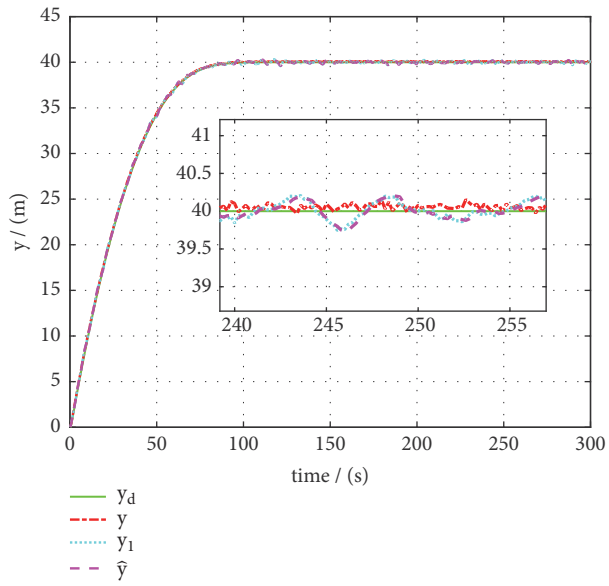

Figure 4: Time history of y-direction position.

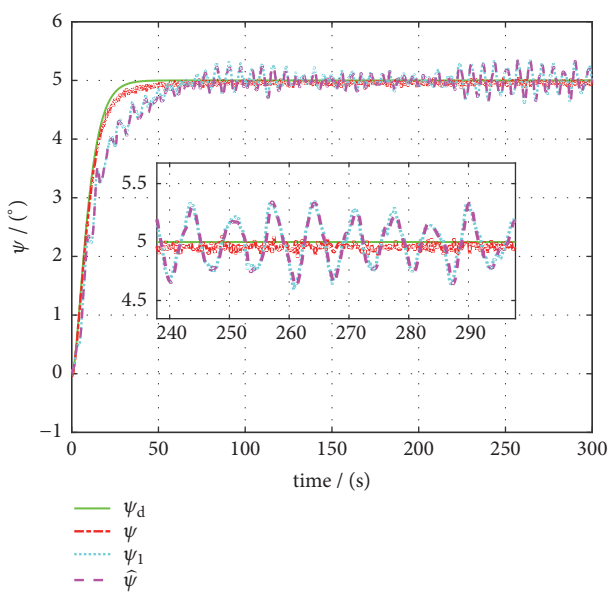

Figure 5: Time history of ψ-direction position.

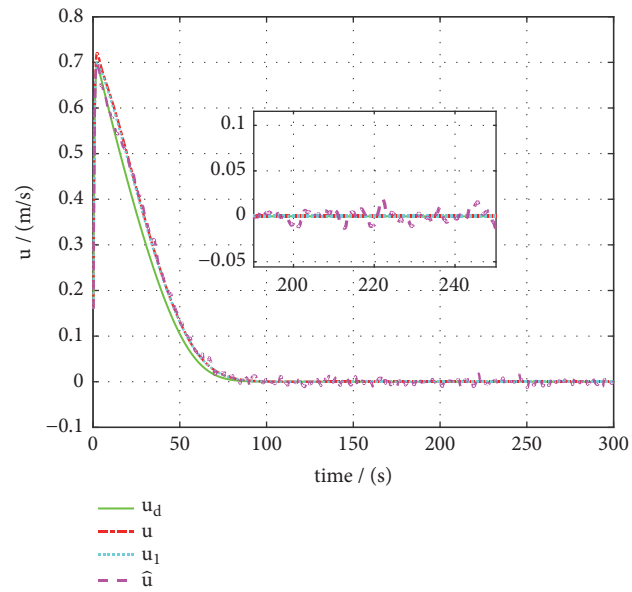

Figure 6: Time history of u-direction velocity.

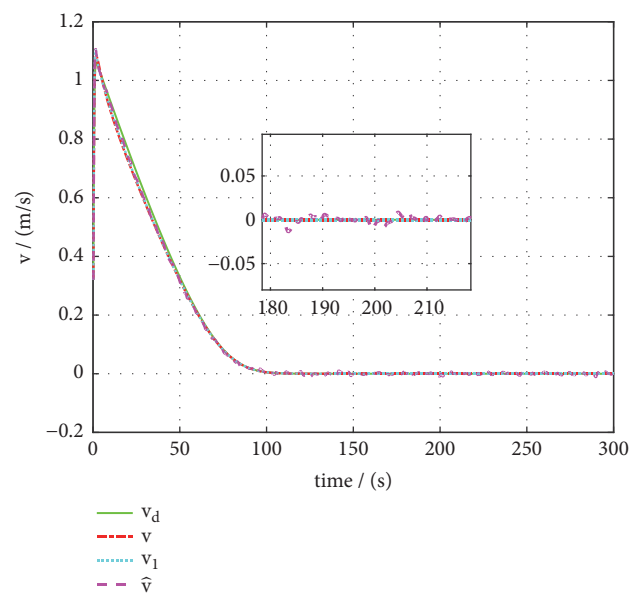

Figure 7: Time history of v-direction velocity.

and maintains the desired position under the effect of environmental disturbances. Thus, the two control objectives are implemented under the control law $\boldsymbol{\tau}_{blf}$. Also position y_1 smoothly and precisely moves to the desired position and maintains the desired position. And the estimated state $\hat{y}$ precisely and smoothly approaches the position in y-direction. But from the partial enlarged details in Figure 4, since the WF motion in y-direction is nonlinear motion and affects the whole motion of ship, the states y, y_1 and estimated state $\hat{y}$ oscillate slightly. However, y under the presented control law $\boldsymbol{\tau}_{blf}$ is smoother and more precise than y_1 under control law $\boldsymbol{\tau}$.

In Figure 5, the heading angle ψ smoothly moves along the desired heading angle ψ_d in the condition of constrained heading angle from $\mathbf{k}_1$ and environmental disturbances and maintains the desired heading angle in the case of constrained heading angle and disturbances. Thus, the two control objectives are implemented under the control law $\boldsymbol{\tau}_{blf}$. Also, the heading angle ψ_1 smoothly moves along the desired heading angle and maintains the desired heading angle. Furthermore, the rising time of ψ_1 is longer than the rising time of ψ. And the estimated state $\hat{\psi}$ smoothly approaches to the heading angle. But from the partial enlarged details in Figure 5, since the WF motion in ψ-direction is nonlinear motion and affects the whole motion of ship, the states ψ, ψ_1 and estimated state

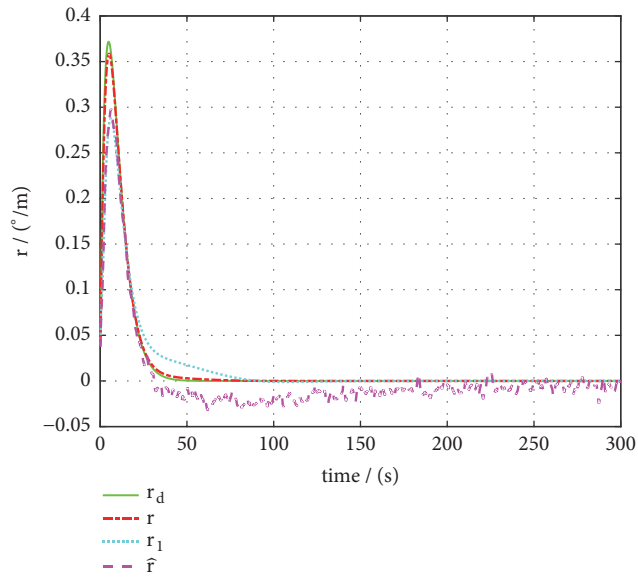

Figure 8: Time history of r-direction velocity.

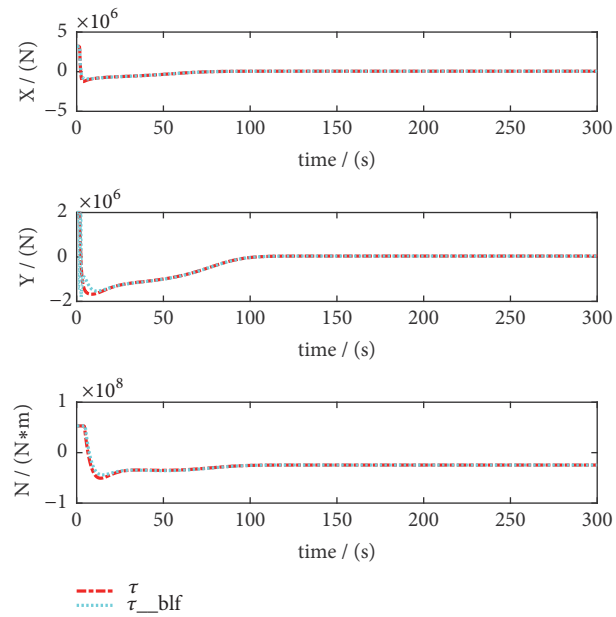

Figure 9: Time history of control forces and moment.

$\hat{\psi}$ oscillate slightly. In this view, ψ under the presented control law $\boldsymbol{\tau}_{blf}$ is faster, smoother, and more precise than ψ_1 under control law $\boldsymbol{\tau}$.

Figures 6, 7, and 8 are velocities in three directions. From Figure 6, the velocities u and u_1 are smoothly and precisely moving along the desired velocity. And the estimated velocity $\hat{u}$ shows slight oscillation in partial enlarged details due to adding the estimation of nonlinear WF velocities in direction of x. With the same condition in Figure 7, the velocities v and v_1 are smoothly and precisely moving along the desired velocity. And the estimated velocity $\hat{v}$ oscillates slightly in partial enlarged details due to adding the estimation of nonlinear WF velocities in direction of y. From Figure 8, the velocities r and r_1 are smoothly moving along the desired velocity r_d. But the top value of velocity r_1 is not arriving at the desired top value of desired velocity. In this view, the velocity r is more precise than r_1. Besides, there are some oscillations in estimated velocity $\hat{r}$ due to adding the estimation of nonlinear WF velocities in ψ-direction.

In addition, the simulation results of control forces and moment in three directions under control laws $\boldsymbol{\tau}_{blf}$ and $\boldsymbol{\tau}$ are shown in Figure 9. The control forces and moment are smoother under the control law $\boldsymbol{\tau}_{blf}$ than control law $\boldsymbol{\tau}$.

Therefore, the position, heading, and velocities under presented control law $\boldsymbol{\tau}_{blf}$ show better performance than traditional control law $\boldsymbol{\tau}$.

6. Conclusions

In this paper, in order to limit the position and heading into certain range for safety reasons, a control law is proposed combining backstepping technique with BLF. Utilizing an error constrained vector in BLF, the virtual control law and backstepping control law are derived to limit the position and heading. And the designed control law is proved stable in the sense of Lyapunov stability theories. The simulation results show that the position and heading under proposed control law move along the desired position and heading in the constrained position, heading, and the effect of environmental disturbances, and maintain the desired position and heading under the constraint position and the effect of environmental disturbances. Therefore, the two control objectives are achieved under the designed control law. And a traditional backstepping control law is also introduced as comparison. Through the comparisons of the two methods, the position and heading appear faster, smoother, and more precise under the proposed control law than traditional control law. Therefore, the proposed control law shows better performance than traditional control law. Moreover, a passive observer is adopted to estimate position and velocities of ship. Considering the nonlinear WF motion of observer, there are small oscillations during control of position, heading angle, and estimation of position and velocities, and the future work is to research this phenomenon.

Data Availability

The authors declare that data sources are public and are referred to in [6, 20] (Xia, G., Xue, J., Jiao, J, 2018, Fossen, T. I, 2002).

Conflicts of Interest

The authors declare that there are no conflicts of interest regarding the publication of this study.

Acknowledgments

This work was supported by the National Natural Science Foundation of China (No. 51609046), the Fundamental Research Funds for the Central Universities

(HEUCFM170403, HEUCFJ180404), and the 7th Generation Ultra Deep Water Drilling Unit Innovation Project.

References

[1] A. J. Sørensen, "A survey of dynamic positioning control systems," *Annual Reviews in Control*, vol. 35, no. 1, pp. 123–136, 2011.

[2] A. J. Sørensen, "Structural Issues in The Design And Operation of Marine Control Systems," *Annual Reviews in Control*, vol. 29, no. 1, pp. 125–149, 2005.

[3] O. M. R. Rabanal, A. H. Brodtkorb, and M. Breivik, "Comparing Controllers for Dynamic Positioning of Ships in Extreme Seas," *IFAC-PapersOnLine*, vol. 49, no. 23, pp. 258–264, 2016.

[4] G. Xia, J. Xue, J. Jiao et al., "Adaptive Fuzzy Control for Dynamic Positioning Ships with Time-Delay of Actuator," in *Proceedings of the 2016 OCEANS MTS/IEEE Monterey, OCE 2016*, pp. 1–6, California, Calif, USA, September 2016.

[5] Y.-S. Kim, J. Kim, and H.-G. Sung, "Weather-Optimal Control of A Dynamic Positioning Vessel Using Backstepping: Simulation And Model Experiment," *IFAC-PapersOnLine*, vol. 49, no. 23, pp. 232–238, 2016.

[6] G. Xia, J. Xue, and J. Jiao, "Dynamic Positioning Control System with Input Time-Delay Using Fuzzy Approximation Approach," *International Journal of Fuzzy Systems*, vol. 20, no. 2, pp. 630–639, 2018.

[7] H. M. Morishita and C. E. S. Souza, "Modified Observer Backstepping Controller for A Dynamic Positioning System," *Control Engineering Practice*, vol. 33, no. 33, pp. 105–114, 2014.

[8] X. Liu and B. Abrahamsen, "Risk Assessment of Riser Operations on DP Drilling Units," in *Proceedings of the ASME 2010 29th International Conference on Ocean, Offshore and Arctic Engineering, OMAE2010*, pp. 823–829, China, June 2010.

[9] Y.-J. Liu and S. Tong, "Barrier Lyapunov Functions-Based Adaptive Control for A Class of Nonlinear Pure-Feedback Systems with Full State Constraints," *Automatica*, vol. 64, pp. 70–75, 2016.

[10] Y.-J. Liu and S. Tong, "Barrier Lyapunov Functions for Nussbaum Gain Adaptive Control of Full State Constrained Nonlinear Systems," *Automatica*, vol. 76, pp. 143–152, 2017.

[11] W. He, Z. Yin, and C. Sun, "Adaptive Neural Network Control of a Marine Vessel With Constraints Using the Asymmetric Barrier Lyapunov Function," *IEEE Transactions on Cybernetics*, vol. 47, no. 7, pp. 1641–1651, 2016.

[12] A. Doria-Cerezo, J. A. Acosta, A. R. Castano et al., "Nonlinear State-Constrained Control. Application to The Dynamic Positioning of Ships," in *Proceedings of the 2014 IEEE Conference on Control Applications, CCA 2014*, pp. 911–916, France, October 2014.

[13] F. Tu, S. S. Ge, Y. S. Choo et al., "Adaptive dynamic positioning control for accommodation vessels with multiple constraints," *IET Control Theory & Applications*, vol. 11, no. 3, pp. 329–340, 2017.

[14] L. Kong, W. He, C. Yang et al., "Adaptive Fuzzy Control for A Marine Vessel with Time-Varying Constraints," *IET Control Theory Applications*, vol. 12, no. 10, pp. 1448–1455, 2018.

[15] J. Ghommam, S. El Ferik, and M. Saad, "Robust Adaptive Path-Following Control of Underactuated Marine Vessel with Off-Track Error Constraint," *International Journal of Systems Science*, vol. 49, no. 7, pp. 1540–1558, 2018.

[16] Z. Zheng, Y. Huang, L. Xie, and B. Zhu, "Adaptive Trajectory Tracking Control of a Fully Actuated Surface Vessel With Asymmetrically Constrained Input and Output," *IEEE Transactions on Control Systems Technology*, vol. 26, no. 5, pp. 1851–1859, 2018.

[17] J. Du, X. Hu, H. Liu, and C. L. Chen, "Adaptive Robust Output Feedback Control for A Marine Dynamic Positioning System Based on A High-Gain Observer," *IEEE Transactions on Neural Networks and Learning Systems*, vol. 26, no. 11, pp. 2775–2786, 2015.

[18] J. Du, X. Hu, M. Krstić et al., "Robust Dynamic Positioning of Ships with Disturbances under Input Saturation," *Automatica*, vol. 73, no. C, pp. 207–214, 2016.

[19] S. V. Svenn, A. H. Brodtkorb, R. Skjetne et al., "Time-Varying Model-Based Observer for Marine Surface Vessels in Dynamic Positioning," *IEEE Access*, vol. 5, pp. 14787–14796, 2017.

[20] T. I. Fossen, *Marine Control Systems-Guidance, Navigation, And Control of Ships, Rigs And Underwater Vehicles, Marine Cybernetics*, Norway, 2002.

[21] T. Zhang, N. Wang, and M. Xia, "Adaptive Neural Output Feedback Control of Stochastic Nonlinear Systems with Unmodeled Dynamics," *Mathematical Problems in Engineering*, vol. 32, no. 1, Article ID 529862, 13 pages, 2015.

[22] B. Ren, S. S. Ge, K. P. Tee et al., "Adative Neural Control for Output Feedback Nonlinear Systems Using A Barrier Lyapunov Function," *IEEE Transactions on Neural Networks and Learning Systems*, vol. 21, no. 8, pp. 1339–1345, 2010.


Advances in Operations Research
Advances in Decision Sciences
Journal of Applied Mathematics
The Scientific World Journal
Journal of Probability and Statistics
International Journal of Mathematics and Mathematical Sciences
Hindawi
Submit your manuscripts at
www.hindawi.com
Journal of Optimization
International Journal of Engineering Mathematics
International Journal of Analysis
Journal of Complex Analysis
Advances in Numerical Analysis
Mathematical Problems in Engineering
International Journal of Differential Equations
Discrete Dynamics in Nature and Society
International Journal of Stochastic Analysis
Journal of Mathematics
Journal of Function Spaces
Abstract and Applied Analysis
Advances in Mathematical Physics